



DOI: 10.34910/MCE.105.11

Long-term properties of cement mortar under compression, tension, and 3-point bending

A. Sprince^a , R. Gailitis^a , L. Pakrastins^{*a} , T. Kozlovskis^a , N. Vatin^b 

^a Riga Technical University, Riga, Latvia

^b Peter the Great St. Petersburg Polytechnic University, St. Petersburg, Russia

*E-mail: leonids.pakrastins@rtu.lv

Keywords: long-term properties, creep, shrinkage, compression, tension, 3-point bending, digital image correlation, PVA fibre, OPC mortar

Abstract. Cement composite long-term property assessment usually is limited to the compression strain state due to the difficulty of performing long-term tests in tension and 3-point bending. This paper shows the difference in long-term properties in compression, tension, and 3-point bending for plain ordinary Portland cement mortar (OPC). The obtained results were compared to reinforced specimen results to determine whether the PVA refibres improve the long-term properties of OPC mortar in various stress-strain conditions. Cylinders, compact tension specimens (CT), and beams – plates were prepared to evaluate material properties and the role of fibre reinforcement in these different stress states. Additionally, to conventional surface-attached strain gauges, 2D-DIC was employed to observe the creep strain of specimens in tension. This paper aim to determine long-term property differences in compression, tension and 3-point bending and, also, to see if low amount PVA fibre incorporation improve long-term properties in previously stated stress-strain states. It was determined that the usage of 1 % of PVA fibres increases creep strains in compression on average by 15 % and reduced by 7 % in tension. It reduces shrinkage strain by 18 % in compression and 8 % in tension. The long-term deflection for the PVA fibre-reinforced specimens are, on average by 55 % higher than for plain OPC mortar specimens in 3-point bending.

1. Introduction

Long-term properties like creep and shrinkage is an essential phenomenon to human-made materials such as concrete. They affect the stress and deformation distribution within concrete structures [1–4]. Concrete creep, and shrinkage strain can influence the lifetime of a concrete structure. It is commonly assumed as a process that leads to increased deformations without significant damage development [3, 5].

Many factors do affect the nature of creep and shrinkage in concrete. The main factors are mixture proportions, curing age, environmental temperature, relative humidity, and applied stress level [1].

Shrinkage is the factor that influences creep strains. It has been discovered that shrinkage strains are caused by capillary pressure in the pore walls, according to capillary tension theory [6–8].

A common way to improve material mechanical properties and restrain creep and shrinkage effects is to use refibre reinforcement. Polymer fibres such as polyvinyl alcohol (PVA) and polypropylene (PP) fibres instead improve fracture toughness and resistance. They do not have significant gains to strength [6, 9–13]. It has been noted that PVA fibres, unlike the PP fibres, better increase ordinary Portland cement mortar (OPC) based material mechanical strength. It turns their brittle behaviour into more ductile. This fibre inclusion is significant to structures that could be subjected to tensile stress [14–19].

Sprince, A., Gailitis, R., Pakrastins, L., Kozlovskis, T., Vatin, N. Long-term properties of cement mortar under compression, tension, and 3-point bending. Magazine of Civil Engineering. 2021. 105(5). Article No. 10511. DOI: 10.34910/MCE.105.11

© Sprince, A., Gailitis, R., Pakrastins, L., Kozlovskis, T., Vatin, N., 2021. Published by Peter the Great St.Petersburg Polytechnic University



This work is licensed under a CC BY-NC 4.0

PVA is considered one of the most promising synthetic fibres for cement composite mechanicals. For the enhancement of cement composite mechanical properties. Some of the advantages of these fibres are ductility, resistance to corrosion, strong bonding with the cement matrix, and low cost. The main benefit of fibre addition is the increase of load-bearing tension capacity. The effect on compressive strength increase from PVA fibre addition can be only unequivocally seen when a more considerable amount of the fibres were used in the cement composite mix. There are also several reports regarding the mentioned effect and an increase of porosity in the structure and, therefore, loss of compressive strength and increase of shrinkage strains. In this case, the bending strength and tensile strength are not affected. Depending on the essential purpose and fibre dimensions, the proper amount of fibre addition is from 0.5 % to 2 % by volume. If the fibres' amount is optional, then even with the relative increase in porosity, the fibres would take care of redistributed stresses in the element [20–24]. It also has to be taken into account that many large scale fibres reduce workability. It has also been claimed that increasing the interaction surface of fibre and matrix by reducing the scale of fibre is an effective way to improve mechanical properties [25].

Long-term properties and especially creep and shrinkage, are essential for concrete at an early age. Internal and external restraints at an early age that appear due to the hydration process can cause internal stress development, leading to premature microcracking [2].

Based on the previous scientific assumptions, the theory of linear visco-elasticity is sufficient for creep deformation modelling. The condition here is that the stresses in concrete have to be limited to a level not higher than 40 % of the concrete compressive strength as it has been required in Eurocode 2 [3].

Most used strain measurement methods employ surface-attached mechanical or electrical gauges that are physically fixed to a test specimen's facet or embedded. In many cases, direct gauge attachment technology can be cumbersome or even irrelevant since a surface-attached gauge usually gives a single measurement along one axis (strictly limited to the gauge length) [26, 27]. Furthermore, in stress states such as tension, the specimen's geometry tends to be more complicated than those in compression or bending. Thus, it requires alternative solutions for trustable gauge attachment methods. To observe the deformation behaviour of an object more complete, non-contact displacement measurement systems of 2D/3D-DIC (Digital Image Correlation for bidirectional/tridirectional displacement measurements respectively) can be applied [28, 29]. Even 2D-DIC ultimately allows precisely measure strains (detectable on the surface of a test specimen) along various axes within a plain. DIC was claimed to be a more cost-effective surface deformation research method than conventional methods in less strict limitations for maximal displacements and versatility of acquired data [28].

2. Materials and Methods

2.1. Materials and specimens

Two different OPC mortar mixes were made using Aalborg white cement. The compositions of mixes are shown in Table 1.

Table 1. Prepared mix compositions.

| Plain OPC mortar | | 1 % PVA fiber-reinforced OPC mortar | |
|--------------------------------|-------------------------------|-------------------------------------|-------------------------------|
| Material | Mass for 1m ³ , kg | Material | Mass for 1m ³ , kg |
| Aalborg Portland cement 52.5 R | 450.00 | Aalborg Portland cement 52.5 R | 450.00 |
| Quartz sand 0.3/2.5 | 900.00 | Quartz sand 0.3/2.5 | 900.00 |
| Water | 180.00 | Water | 180.00 |
| Plasticizer VINPLAST CL 10 | 3.60 | Plasticizer VINPLAST CL 10 | 3.60 |
| PVA fibres | – | PVA fibers | 15.79 |
| W/C | 0.40 | W/C | 0.40 |

Three groups of specimens were prepared. For strain of creep in compression and shrinkage strain determination, Ø 46 × 250 mm cylinders were made. The cube was prepared with dimensions 150 × 150 × 150 mm and later was cut into CT plates for strain in tension and shrinkage strain determination. For displacement determination in a 3-point bending, the plate was designed with dimensions 500 × 500 × 20 mm and subsequently was cut into beam specimens. All the specimens were unmolded 24 hours after casting and were submerged in water for four days. On the 5th day, specimen preparation for long-term property tests was started.

2.2. Test specimen preparation

When cylinders were unmolded, they were $\varnothing 46 \times 250$ mm. Specimens at the age of 5 days were cut according to RILEM code requirements for long-term testing in compression [30]. For this necessity, specimens were cut to the length of 194 mm approximately. Their top and bottom faces were ground. Specimen height was 190 mm, and top and bottom plains were perpendicular to the specimen's longitudinal axes. The diameter to height ratio was approximately 1/4.

Afterwards, the specimens intended for creep strain six aluminium plates (10 × 15 mm) were glued on. One aluminium plate was glued on the top and bottom for specimens intended for shrinkage strain measurements. For shrinkage intended specimens, aluminium plates were glued in the middle of the specimen upper and bottom parts and then in the centre [31].

For long-term property testing in tension, compact tension (CT) specimens were used [32]. Each cube was cut into 15 mm thick CT plates. According to Fig. 1, the notch was sawn, and the holes were drilled.

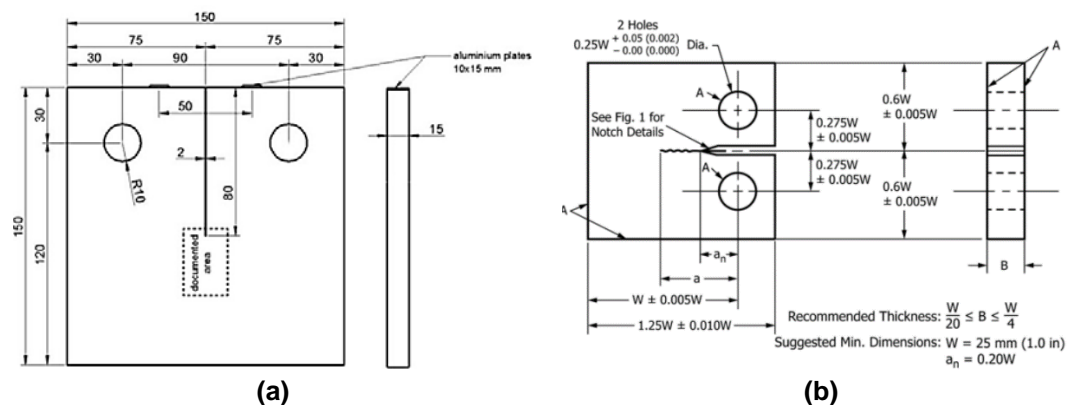


Figure 1. Geometry of the Compact Tension (CT) specimen [31, 32].

The notch in the specimen was sawn by Proxxon MICRO MBS 240/E bandsaw and was 2 mm wide. According to Fig. 1, 2 aluminium plates were glued to the specimen's facet on both sides of the notch. Additionally, the black paint speckle pattern was created on the surface of 2D-DIC specimens.

For the long-term property testing in 3-point bending, each plate was cut into 20 × 75 × 450 mm pieces. The thickness to length ratio is 0.044 [11, 33].

There were 20 cylinders, 5 CT specimens, and 6 beam-plate specimens for each prepared mortar mix.

2.3. Experimental setup

When all the specimens were prepared, the compressive strength, tensile strength, and ultimate load value in 3-point bending were determined. The procedure is shown in Fig. 2, and the results are compiled in Table 2.



a) Compressive ultimate load determination



b) Tensile ultimate load determination



c) 3-point bending ultimate load determination

Figure 2. Experimental test setups for the determination of ultimate load values.

Afterwards, specimens were placed on their test stands. Compression and tension specimens were placed in the creep lever test stands, but 3-point bending specimens were placed in the deflection test

stand (see Fig. 3). Additionally, to a mechanical strain gauge, a single digital SLR camera was placed facing a CT specimen to acquire displacement images that were later processed using commercial software (developed by GOM GmbH). In compression and tension, specimens were loaded with 20 % of the compressive/tensile ultimate load value, whereas 3-point bending 40 % of the ultimate load value. The specimens were loaded as previously described to be within the linear strain state [3].

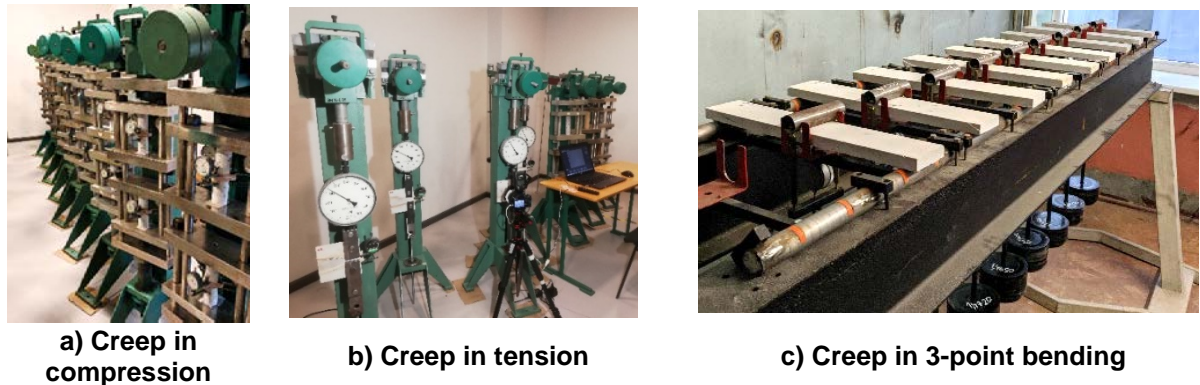


Figure 3. Creep specimens placement in the test stands.

For creep in compression and 3-point bending and shrinkage measurements for all specimens, strain gauges were used with an error margin of +/- 0.01 mm. For creep in tension, digital strain gauges were used with an error margin of +/- 0.001 mm. For the operating principles of the creep lever test stand, see Fig. 4. All specimens were kept in a dry atmosphere of controlled relative humidity in standard conditions: temperature 20 ± 1 °C and relative humidity 30 ± 7 %.

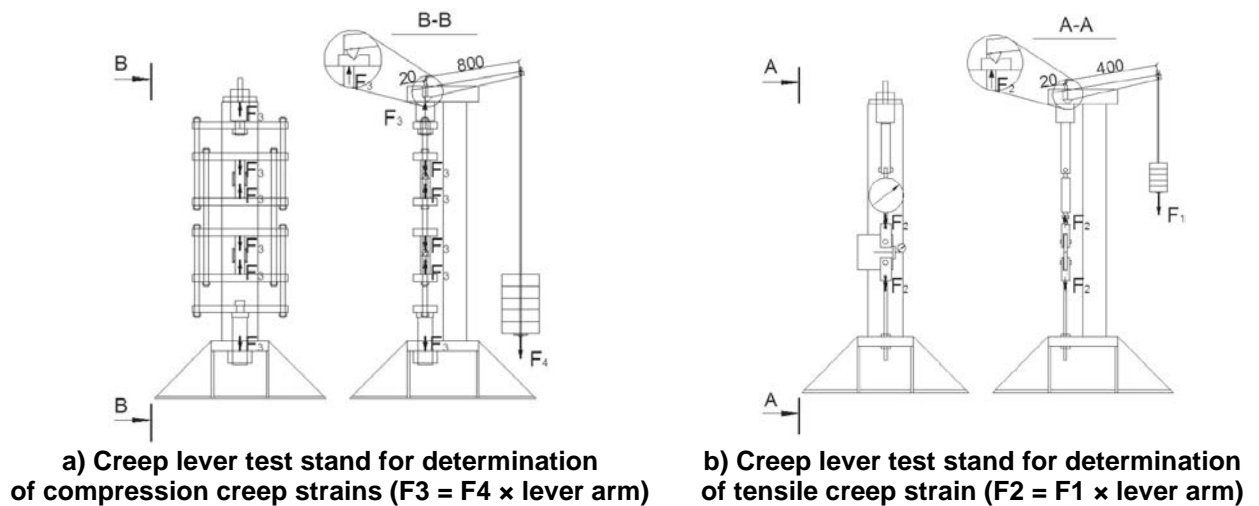


Figure 4. Compression (a) and tension (b) creep lever test stand schemes.

Simultaneously to creep strain tests also shrinkage strain measurements of compression and tension specimens were carried out. The test setup for both strain measurements is shown in Fig. 5.

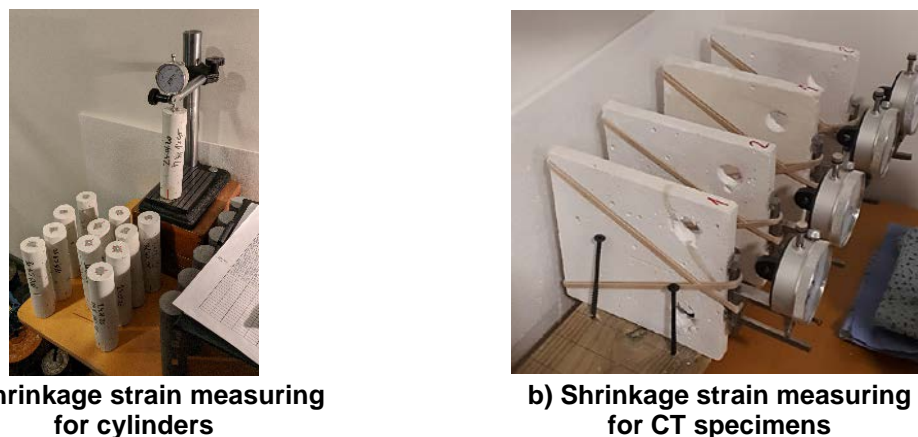


Figure 5. Shrinkage specimen placement in the test stands.

3. Results and Discussion

Before the creep tests, the specimen compressive, tensile, and bending ultimate load values were determined. The obtained results are shown in Table 2.

Table 2. Ultimate load values for all tested specimen types.

| Test type | Specimen type | Average ultimate load, kN |
|-----------------|------------------|---------------------------|
| Compression | Plain OPM | 61.2 |
| | OPM with 1 % PVA | 61.0 |
| Tension | Plain OPM | 0.32 |
| | OPM with 1 % PVA | 0.34 |
| 3-point bending | Plain OPM | 0.27 |
| | OPM with 1 % PVA | 0.30 |

According to these values, the amount of load was calculated that creep specimens were loaded in their test stands.

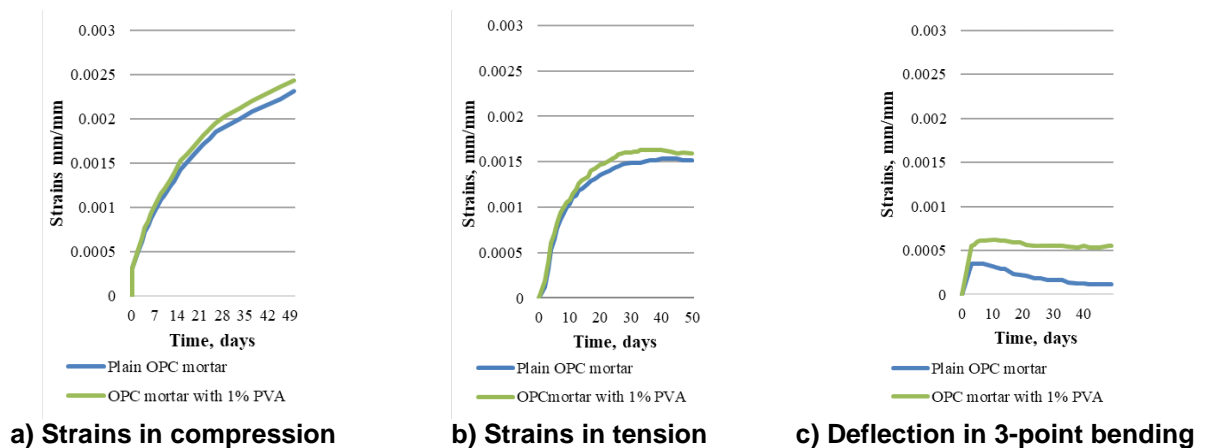


Figure 6. Full strains in compression, tension, and full deflection in 3-point bending.

Fig. 6 shows the curves of the deformations that have been measured for specimens that have not been wrapped in any way to prevent moisture evaporation from the specimen in any way. The fibre-reinforced mortar reached higher strains than plain OPC mortar. Long-term property caused strains to PVA fibre-reinforced specimens to increase around 12 days of testing in compression and tension. Still, in 3-point bending, the deflection of PVA fibre reinforced specimens overcomes plain OPC mortar specimens in the elastic state. The difference between plain and PVA fibre-reinforced specimen strains at its peak in compression is 9.1 % but in tension 8.6 %. The only positive effect of PVA reinforcement – the specimens had more significant elastic strains than plain specimens. As shown in Fig. 8 (a) and (b), the reinforced specimens in cases of compression and tension when loaded had small differences in immediate strains. Still, when unloaded, the difference is much more visible. In 3-point bending, the deflection differences between plain and PVA fibre-reinforced mortar were much more significant.

To get a more thorough look at the creep and shrinkage impact in the specimens loaded in compression and tension in Fig. 7 (a) and (b) is shown curves of creep with and without shrinkage strain part.

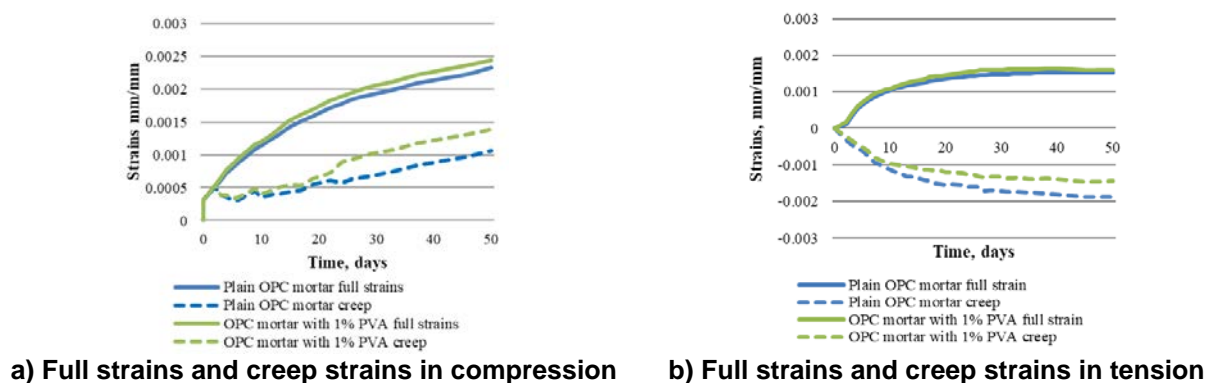


Figure 7. Full strains and creep strains in compression and tension.

Fig. 7 shows that the shrinkage effect of compression and tension specimens is reasonably different. It is possibly due to the specimens' shape and the ability to move the moisture through the specimens. In contrast to Fig. 7 (a) shown long-term properties and raw creep strains in compression, the curves in Fig. 7 (b) representing long-term properties and raw creep in tension show that the shrinkage effect to the tension specimens is significantly higher than for the compression specimens. The creep curves in tension are with downward characteristics, unlike compression creep specimens. Curves show that tension creep was opening the notch, but shrinkage (Fig. 8b) tightens and close down the notch with more significant effort. The mean value of creep curves in tension is around 2 % smaller than those in compression. The shrinkage mean value, in contrast, to creep in tension is 41 %.

In this research work, the use of 2D-DIC application aimed to obtain experimental data of cement composite creep data and conclude whether this method's usage is suitable for such application. According to the authors' knowledge, DIC is not widely used in long-term tests as a measuring tool. Obtained strain data of specimens in tension show close similarity with conventionally registered (using surface-attached gauges) results. Characteristics of graph curves correspond, but numerical data closely deviate since a virtual strain gauge cannot be applied entirely at the same spot as a mechanical system.

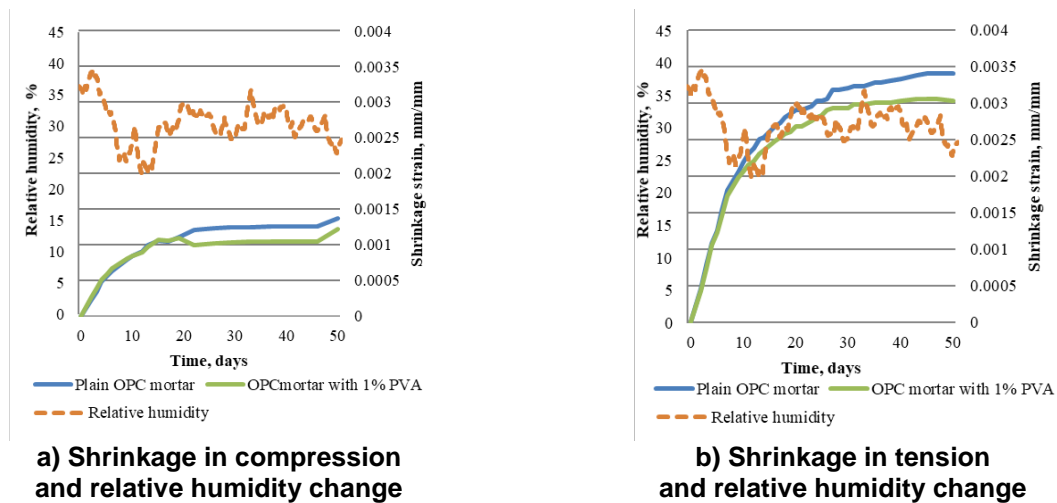


Figure 8. Shrinkage strains in compression and tension and relative humidity change.

In further, analyze shrinkage strains in compression (Fig. 8 (a)) and tension (Fig. 8 (b)) and the strain dependence from changes in relative humidity. In that case, specimens in compression react to humidity changes more rapidly than specimens in tension. Furthermore, compression specimens have very rapid strain characteristics when the moisture content increases, unlike tension specimens. For tension specimens, the strain changes from humidity level changes were more aimed to seek a balance point for specimen when the humidity level in the environment matches in the specimen. Then it would slowly react to humidity changes and deform. Farah M et al. [2] stated that creep testing for concrete at an early age leads to high creep displacements due to shrinkage and water movement into the concrete. Also, the shrinkage amount in compression is significantly less than in tension. The difference in peak shrinkage values is 70.5 % higher in tension. Fig. 6 to Fig. 8 fully shows this statement.

To further analyze obtained creep curves, the elastic strains at the beginning of the testing were taken away to evaluate raw creep strains. These curves are shown in Fig. 9.

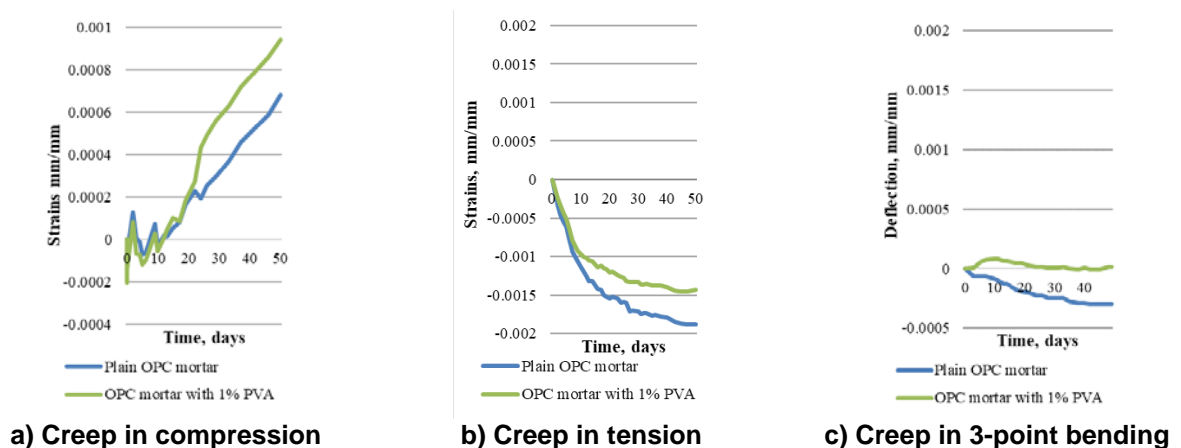


Figure 9. Creep strains without elastic strain part.

Fig. 9 clearly shows that mean creep values are close and within a 5 % margin in general in compression and tension. It has to be mentioned that the 1 % PVA fiber-reinforced OPC mortar specimens show higher strains in compression than in tension and vice versa for plain OPC mortar. The difference here is 17.89 % and 20.21 % for PVA fiber-reinforced and plain OPC mortar correspondingly. The strains in 3-point bending in contrast to strains in compression and tension are significantly less and at peak value is only about 25 % from the highest strain value in tension (plain OPC mortar specimens).

The further see moisture influence to the mortar mechanical properties. Half of the specimens were subjected to water saturation for 24 hours. The results are shown in Table 3 and Table 4.

Table 3. Water absorption characteristics of specimens.

| Specimen type | Specimen mix type | Average weight before H ₂ O, kg | Average weight after 24 hours in H ₂ O, kg | Average absorbed H ₂ O weight, kg |
|---|-------------------|--|---|--|
| Cylinder specimen of creep in compression | 1 % PVA | 0.6483 | 0.6878 | 0.0395 |
| | Plain | 0.6468 | 0.6858 | 0.0390 |
| Cylinder specimen of shrinkage | 1 % PVA | 0.6455 | 0.6865 | 0.0410 |
| | Plain | 0.6693 | 0.7093 | 0.0400 |
| CT specimen of creep in tension | 1 % PVA | 0.5065 | 0.5540 | 0.0475 |
| | Plain | 0.6070 | 0.6530 | 0.0460 |
| CT specimen of shrinkage | 1 % PVA | 0.5585 | 0.6075 | 0.0490 |
| | Plain | 0.6465 | 0.6965 | 0.0500 |
| Beam-plate specimen of creep in 3-point bending | 1 % PVA | 1.4065 | 1.4820 | 0.0755 |
| | Plain | 1.4620 | 1.5425 | 0.0805 |

As shown in Table 3, whether the specimen has been loaded does not significantly affect the water absorption ability. The difference of same mix specimen water absorption differing from the test they had been subjected to is within 4 % margin for specimens that were used to test creep and shrinkage in compression. Within 8 % for specimens used to test creep and shrinkage in tension and within 5 % for specimens used to test creep in 3-point bending. A shrinkage test in 3-point bending was not conducted.

Table 4. Water absorption effect to ultimate load.

| Specimen type | Specimen mix type | Average strength for air-dry specimens, kN | Average strength for water-saturated specimens, kN | Average strength loss due to water saturation, % |
|---|-------------------|--|--|--|
| Cylinder specimen of creep in compression | 1 % PVA | 70.1 | 49.8 | 29.06 |
| | Plain | 72.9 | 43.1 | 41.88 |
| Cylinder specimen of shrinkage | 1 % PVA | 53.2 | 43.5 | 18.24 |
| | Plain | 63.4 | 38.7 | 39.96 |
| CT specimen of creep in tension | 1 % PVA | 0.38 | 0.35 | 7.89 |
| | Plain | 0.46 | 0.39 | 15.22 |
| CT specimen of shrinkage | 1 % PVA | 0.46 | 0.40 | 13.04 |
| | Plain | 0.55 | 0.38 | 30.91 |
| Beam-plate specimen of creep in 3-point bending | 1 % PVA | 0.305 | 0.225 | 26.23 |
| | Plain | 0.320 | 0.220 | 31.25 |

From Table 4, it becomes clear that loaded specimens have significantly higher compressive load than the ones that have been used as shrinkage specimens (without load). As stated previously, when the compressive strength values for creep tests were determined, the 1 % PVA fibre incorporation into the mix did not show immediate improvement to the mechanical properties in compression. The only slight improvement that becomes apparent was that when specimens were subjected to water for 24 hours, then for those specimens, the loss of ultimate compressive load was from 12.82 to 21.72 % lower than for the plain OPC mortar. In the air-dry state difference between compressive load values to specimens are 4.9 and 16.1 %, but in water-saturated, this difference favours the PVA fibre-reinforced specimens 15.5 and 11.1 %, respectively. A similar tendency is apparent with tension and 3-point bending specimens. The PVA fibre-reinforced specimens have from 4.6 % lower bending strength load up to 17.4 % maximum tensile load in the air-dry state than plain specimens. Water-saturated PVA fibre-reinforced specimens showed a different situation when PVA reinforced specimens show more considerable ultimate tension and bending

load values than plain specimens. The decline of the maximum load value for PVA fibre-reinforced specimens is significantly less than the plain mortar ones. In general, it seems that 1 % PVA fibre by weight addition does not only decrease compressive strength as J.J. Ekaputri et al. and J. Topic et al. [34, 35] had stated but also the decrease in tensile strength as well.

If the values in Table 2 and Table 4 were compared, the plain specimens that were not subjected to load had increased their compressive strength, but PVA fiber-reinforced had lost it. It can be due to the nature of fibre reinforcement and uneven fibre distribution in the specimen. All of the loaded specimen compressive load values had risen significantly and are 16.1 and 13.0 % higher for plain and PVA fibre-reinforced ones, respectively.

4. Conclusions

This article's main primary purpose is to determine the difference of long-term strains in compression, tension and 3-point bending to OPC mortar with and without PVA fibre reinforcement. The overall conclusions are:

- In compression specimens with 1 % PVA fibre, it only improves compressive strength in a water-saturated state and is 11 to 13.5 %. In other cases, specimens show from 3.8 to 10.2 % less compressive strength than plain OPC mortar specimens;
- Initially, tension specimens with 1 % PVA fibres show higher tensile strength than plain OPC mortar specimens. After long-term testing, specimens with fibres show superior strength in tension only when the specimens were wet. At the beginning of testing, air dry PVA fibre specimens were 5.9 % resistant to tension, but plain specimens show from 16.4 to 17.4 % higher strength in tension at the end of testing. In a water-saturated state, plain specimens that have been tested to creep show 12.8 % higher strength in tension, but shrinkage test PVA fibre-reinforced specimens show 5 % higher strength in tension than plain OPC mortar specimens;
- For specimens that were used in the 3-point bending, the strength situation is similar to tension specimens. At the beginning of testing, specimens are 10 % with a higher strength than plain OPC mortar specimens. Still, after testing plain specimens in the air-dry state, they show a 4.7 % maximum load value. In water saturate state, fibre-reinforced specimens show a 2.2 % higher ultimate load value;
- Specimens with PVA fibre reinforcement show less strength loss due to water saturation than plain OPC mortar specimens. On average, it is 23.65 % and 40.92 % in compression for PVA and plain specimens, 10.47 % and 23.07 % in tension for PVA and plain OPC mortar specimens 26.23 % and 31.25 % in three-point bending for PVA and plain specimens correspondingly;
- Creep strains in tension and creep deflection in 3-point bending specimens with PVA fibres are reduced than without them. The creep strains are, on average, 21 % larger than plain OPC mortar specimens with a peak difference of 25 % in compression. The increase of creep strains in tension is less, but PVA fibre specimens on average show 7 % higher strains with a peak value of 29 % in the early loading stages. In 3-point bending, the long-term strains are on average 55 % less to the plain OPC mortar specimens with a peak value of 73 % in the late stages of loading. In compression, it is the other way around, with the increase in creep for the PVA fibre-reinforced specimens by 15.2 % at the peak;
- In shrinkage specimens with PVA, fibres show their superiority – in compression strains. PVA fibre specimens are on average 18 % less with a peak value of 42 % in late testing stages. The superiority is only 8 % to plain OPC mortar specimens with its peak value of 29 % in the late testing stages in tension;
- The 2D-DIC displacement measuring system is well applicable to monitor the creep behaviour of cement composite materials.

For further research, it is planned to have the same test procedure as it was described in this article. The test subject would be geopolymer composite. The results would then be compared with the results obtained in this article and determined whether geopolymer composite holds significantly better long-term properties at an early age.

5. Acknowledgements

This work has been supported by the Latvian Council of Science within the scope of the project 'Long term properties of innovative cement composites in various stress-strain conditions' No. lzp-2018/2-0249.

This publication was supported by Riga Technical University's Doctoral Grant programme.

This work has been supported by the European Regional Development Fund within the Activity 1.1.1.2 "Post-doctoral Research Aid" of the Specific Aid Objective 1.1.1 "To increase the research and innovative capacity of scientific institutions of Latvia and the ability to attract external financing, investing in human resources and infrastructure" of the Operational Programme "Growth and Employment" (No.1.1.1.2/VIAA/3/19/401).

Conflicts of Interest: The authors declare no conflict of interest.

References

- Liang, S., Wei, Y. Methodology of obtaining intrinsic creep property of concrete by flexural deflection test. *Cement and Concrete Composites*. 2019. 97 (April 2018). Pp. 288–299. DOI: <https://doi.org/10.1016/j.cemconcomp.2019.01.003>
- Farah, M., Grondin, F., Alam, S.Y., Loukili, A. Experimental approach to investigate creep-damage bilateral effects in concrete at early age. *Cement and Concrete Composites*. 2019. 96 (November 2018). Pp. 128–137. DOI: <https://doi.org/10.1016/j.cemconcomp.2018.11.022>
- Boumakis, I., Di Luzio, G., Marcon, M., Vorel, J., Wan-Wendner, R. Discrete element framework for modeling tertiary creep of concrete in tension and compression. *Engineering Fracture Mechanics*. 2018. 200(July). Pp. 263–282. DOI: <https://doi.org/10.1016/j.engfracmech.2018.07.006>
- Rossi, P., Tailhan, J.L., Le Maou, F. Comparison of concrete creep in tension and in compression: Influence of concrete age at loading and drying conditions. *Cement and Concrete Research*. 2013. 51. Pp. 78–84. DOI: <http://dx.doi.org/10.1016/j.cemconres.2013.04.001>
- Ibragimov, R., Fediuk, R. Improving the early strength of concrete: Effect of mechanochemical activation of the cementitious suspension and using of various superplasticizers. *Construction and Building Materials*. 2019. 226. Pp. 839–848. DOI: <https://doi.org/10.1016/j.conbuildmat.2019.07.313>
- Nizina, T.A., Balykov, A.S. Experimental-statistical models of properties of modified fiber-reinforced fine-grained concretes. *Magazine of Civil Engineering*. 2016. 62(2). Pp. 13–25. DOI: 10.5862/MCE.62.2
- Lee, N.K., Jang, J.G., Lee, H.K. Shrinkage characteristics of alkali-activated fly ash/slag paste and mortar at early ages. *Cement and Concrete Composites*. 2014. 53. Pp. 239–248. DOI: <http://dx.doi.org/10.1016/j.cemconcomp.2014.07.007>
- Kuenzel, C., Li, L., Vandeperre, L., Boccaccini, A.R., Cheeseman, C.R. Influence of sand on the mechanical properties of metakaolin geopolymers. *Construction and Building Materials*. 2014. 66. Pp. 442–446. DOI: 10.1016/j.conbuildmat.2014.05.058
- Falliano, D., De Domenico, D., Ricciardi, G., Gugliandolo, E. Compressive and flexural strength of fiber-reinforced foamed concrete: Effect of fiber content, curing conditions and dry density. *Construction and Building Materials*. 2019. 198. Pp. 479–493. DOI: <https://doi.org/10.1016/j.conbuildmat.2018.11.197>
- Vrijdaghs, R., di Prisco, M., Vandewalle, L. Creep of polymeric fiber reinforced concrete: A numerical model with discrete fiber treatment. *Computers and Structures*. 2020. 233. Pp. 106233. DOI: <https://doi.org/10.1016/j.compstruc.2020.106233>
- Das, C.S., Dey, T., Dandapat, R., Mukharjee, B.B., Kumar, J. Performance evaluation of polypropylene fibre reinforced recycled aggregate concrete. *Construction and Building Materials*. 2018. 189. Pp. 649–659. DOI: <https://doi.org/10.1016/j.conbuildmat.2018.09.036>
- Amran, M., Fediuk, R., Vatin, N., Lee, Y.H., Murali, G., Ozbakkaloglu, T., Klyuev, S., Alabduljabber, H. Fibre-reinforced foamed concretes: A review. *Materials*. 2020. 13(19). Pp. 1–36. DOI: 10.3390/ma13194323
- Fediuk, R.S., Klyuev, A.V., Liseitsev, Y.L., Timokhin, R.A. Fiber concrete on greenest cementitious binders for road construction. *Lecture Notes in Civil Engineering*. 2021. 95. Pp. 143–149.
- Afroughsabet, V., Teng, S. Experiments on drying shrinkage and creep of high performance hybrid-fiber-reinforced concrete. *Cement and Concrete Composites*. 2020. 106(November 2019). Pp. 103481. DOI: <https://doi.org/10.1016/j.cemconcomp.2019.103481>
- Liu, F., Ding, W., Qiao, Y. Experimental investigation on the tensile behavior of hybrid steel-PVA fiber reinforced concrete containing fly ash and slag powder. *Construction and Building Materials*. 2020. 241. Pp. 118000. DOI: <https://doi.org/10.1016/j.conbuildmat.2020.118000>
- Paegle, I., Minelli, F., Fischer, G. Cracking and load-deformation behavior of fiber reinforced concrete: Influence of testing method. *Cement and Concrete Composites*. 2016. 73. Pp. 147–163. DOI: <http://dx.doi.org/10.1016/j.cemconcomp.2016.06.012>
- Pupure, L., Varna, J., Joffe, R., Berthold, F., Miettinen, A. Mechanical properties of natural fiber composites produced using dynamic sheet former. *Wood Material Science and Engineering*. 2020. 15(2). Pp. 76–86. DOI: 10.1080/17480272.2018.1482368
- Klyuev, S., Klyuev, A., Vatin, N. Fine-grained concrete with combined reinforcement by different types of fibers. *MATEC Web of Conferences*. 2018. 245. DOI: 10.1051/mateconf/201824503006
- Fediuk, R., Mochalov, A., Timokhin, R. Review of methods for activation of binder and concrete mixes. *AIMS Materials Science*. 2018. 5(5). Pp. 916–931. DOI: 10.3934/mat.2018.5.916
- Said, M., Abd El-Azim, A.A., Ali, M.M., El-Ghazaly, H., Shaaban, I. Effect of elevated temperature on axially and eccentrically loaded columns containing Polyvinyl Alcohol (PVA) fibers. *Engineering Structures*. 2020. 204 (December 2019). Pp. 110065. DOI: <https://doi.org/10.1016/j.engstruct.2019.110065>
- Ling, Y., Zhang, P., Wang, J., Chen, Y. Effect of PVA fiber on mechanical properties of cementitious composite with and without nano-SiO₂. *Construction and Building Materials*. 2019. 229. Pp. 117068. DOI: <https://doi.org/10.1016/j.conbuildmat.2019.117068>
- Wang, J., Dai, Q., Si, R., Guo, S. Investigation of properties and performances of Polyvinyl Alcohol (PVA) fiber-reinforced rubber concrete. *Construction and Building Materials*. 2018. 193. Pp. 631–642. DOI: <https://doi.org/10.1016/j.conbuildmat.2018.11.002>
- Noushini, A., Samali, B., Vessalas, K. Effect of polyvinyl alcohol (PVA) fibre on dynamic and material properties of fibre reinforced concrete. *Construction and Building Materials*. 2013. 49. Pp. 374–383. DOI: <http://dx.doi.org/10.1016/j.conbuildmat.2013.08.035>
- Liu, F., Ding, W., Qiao, Y. Experimental investigation on the flexural behavior of hybrid steel-PVA fiber reinforced concrete containing fly ash and slag powder. *Construction and Building Materials*. 2019. 228. Pp. 116706. DOI: <https://doi.org/10.1016/j.conbuildmat.2019.116706>

25. Ranjbar, N., Mehrali, M., Mehrali, M., Alengaram, U.J., Jumaat, M.Z. High tensile strength fly ash based geopolymer composite using copper coated micro steel fiber. *Construction and Building Materials*. 2016. 112. Pp. 629–638. DOI: <http://dx.doi.org/10.1016/j.conbuildmat.2016.02.228>
26. Biscaia, H., Franco, N., Chastre, C. Stainless Steel Bonded to Concrete: An Experimental Assessment using the DIC Technique. *International Journal of Concrete Structures and Materials*. 2018. 12(1). DOI: 10.1186/s40069-018-0229-8
27. del Rey Castillo, E., Allen, T., Henry, R., Griffith, M., Ingham, J. Digital image correlation (DIC) for measurement of strains and displacements in coarse, low volume-fraction FRP composites used in civil infrastructure. *Composite Structures*. 2019. 212. Pp. 43–57. DOI: 10.1016/j.compstruct.2019.01.024
28. Smrkíć, M.F., Koščak, J., Damjanović, D. Application of 2D digital image correlation for displacement and crack width measurement on RC elements. *Gradjevinar*. 2018. 70(9). Pp. 771–781. DOI: 10.14256/JCE.2407.2018
29. A Good Practices Guide for Digital Image Correlation Standardization, Good Practices, and Uncertainty Quantification Committee. 2018. DOI: 10.32720/idics/gpg.ed1/print.format
30. Acker, P., Agullo, L., Auperin, M., Carol, I., J. Carreira, D., M.R. Catarino, J., Chem, J.-C., A. Chiorino, M., W. Dougill, J., Huet, C., Kanstad, T., Kim, J.-K., Křístek, V., Republic, C., S. Muller, H., Byung, G., Oh, H., Ožbolt, J., Reid, S., Wittmann, F. RILEM TC 107-CSP: CREEP AND SHRINKAGE PREDICTION MODELS: PRINCIPLES OF THEIR FORMATION Recommendation Measurement of time-dependent strains of concrete. *Materials and Structures*. 1998. 31. Pp. 507–512.
31. Sprince, A., Pakrastins, L., Baskers, B., Gaile, L. Crack development research in extra fine aggregate cement composites. *Vide. Tehnologija. Resursi – Environment, Technology, Resources*. 2015. 1. Pp. 205–208. DOI: 10.17770/etr2015vol1.199
32. ASTM. E647 – Standard Test Method for Measurement of Fatigue Crack Growth Rates. *ASTM Book of Standards*. 2016. 03(July). Pp. 1–49. DOI: 10.1520/E0647-15E01.2
33. Ranaivomanana, N., Multon, S., Turatsinze, A. Basic creep of concrete under compression, tension and bending. *Construction and Building Materials*. 2013. 38. Pp. 173–180. DOI: <http://dx.doi.org/10.1016/j.con-buildmat.2012.08.024>
34. Ekaputri, J.J., Limantono, H., Triwulan, Susanto, T.E.S., Abdullah, M.M.A.B. Effect of PVA fiber in increasing mechanical strength on paste containing glass powder. *Key Engineering Materials*. 2016. 673(August). Pp. 83–93. DOI: 10.4028/www.scientific.net/KEM.673.83
35. Topic, J., Prošek, Z., Indrová, K., Plachý, T., Nežerka, V., Kopecký, L., Tesárek, P. Effect of PVA modification on the properties of cement composites. *Acta Polytechnica*. 2015. 55(1). Pp. 64–75. DOI: 10.14311/AP.2015.55.0064

Contacts:

Andina Sprince, Andina.Sprince@rtu.lv

Rihards Gailitis, rihards.gailitis@rtu.lv

Leonids Pakrastins, leonids.pakrastins@rtu.lv

Tomass Kozlovskis, tomass.kozlovskis@rtu.lv

Nikolai Vatin, vatin@mail.ru